Science of the Total Environment 778 (2021) 146242

Contents lists available at ScienceDirect

Science of the Total Environment

journal homepage: www.elsevier.com/locate/scitotenv

The black carbon dispersion in the Southern Hemisphere and its transport and fate to Antarctica, an Anthropocene evidence for climate change policies

Ernesto Pino-Cortés [a,*], Luis A. Díaz-Robles [b], Francisco Cubillos [b], Francisco Cereceda-Balic [c], Roberto Santander [b], Joshua S. Fu [d,e], Samuel Carrasco [a], Jonathan Acosta [f]

[a] Escuela de Ingeniería Química, Pontificia Universidad Católica de Valparaíso, Ave Brasil 2162, Valparaíso, Chile
[b] Departamento de Ingeniería Química, Universidad de Santiago de Chile, Ave Libertado Bernardo O'Higgins 3363, Santiago de Chile, Chile
[c] Centre for Environmental Technologies and Department of Chemistry, Universidad Técnica Federico Santa María, Avenida España 1680, Valparaíso, Chile
[d] Department of Civil and Environmental Engineering, University of Tennessee, 851 Neyland Drive, Knoxville, TN, USA
[e] Computational Earth Sciences Group, Computational Science and Engineering Division, Oak Ridge National Laboratory, 1 Bethel Valley Road, Oak Ridge, TN, USA
[f] Departamento de Estadística, Pontificia Universidad Católica de Chile, Avenida Vicuña Mackenna 4860, Santiago de Chile, Chile

HIGHLIGHTS

- Simulation of the long range transportation of atmospheric black carbon.
- The biomass burning is the main responsible of the atmospheric black carbon in Antarctica.
- West Antarctica is impacted in 17–24 days since black carbon is emitted.

GRAPHICAL ABSTRACT

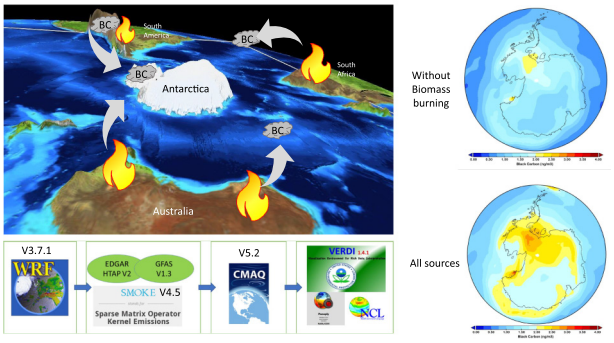

ARTICLE INFO

Article history:
Received 17 December 2020
Received in revised form 26 February 2021
Accepted 27 February 2021
Available online 10 March 2021

Editor: Philip K. Hopke

Keywords:
Black carbon
CMAQ
Antarctica
Biomass burning
Anthropogenic sources
Hemispheric simulation

ABSTRACT

Black carbon (BC) has been measured in Antarctica's air, and its global warming effect can potentially speed up the ice melting in the most solid water reservoir of the planet. However, the primary responsible sources are not well evidenced in this region. The dispersion of black carbon emissions from the Southern Hemisphere was conducting using atmospheric chemical transport model and we compared the results with satellite registries from March 1st to April 30th in 2014. The emission inventory considered the anthropogenic and biomass burning emissions from global datasets. The largest and most populated cities in Southern Hemisphere showed the higher emission of BC. As a result, the average daily concentrations of atmospheric BC were around 4 ng/m^3 in most regions of Antarctica according to its pristine characteristics. We analyzed fifteen relevant sites in coastal zones of Antartica and some peaks registered by the satellite records were not replicated by model outputs and it was mainly associated with the lack of emissions. Finally, we made simulations in the same period without biomass burning emissions and we observed decreased concentrations of BC in the range of 20–50%. As a result, we show that the black carbon transportation from the continental land to the polar region took place in 17–24 days during the Austral summer and the biomass burning emissions were the primary source. Black Carbon deposition in Antarctica is not permanent, but the uncontrolled emissions from Southern Hemisphere can increase its transportation to the white continent and make its accumulation during the period when the weak polar vortex occurs.

* Corresponding author.
E-mail address: ernesto.pino@pucv.cl (E. Pino-Cortés).

https://doi.org/10.1016/j.scitotenv.2021.146242
0048-9697/

1. Introduction

Air pollution is one of the biggest problems that humankind faces today. Higher emissions of pollutants from several chemical reactions on natural and anthropogenic sources have generated several environmental problems at local and regional scales. Black carbon (BC) is one of the substances with many studies related to this topic. It is well known generated from incomplete combustion of biomass and fossil fuels (Petzold et al., 2013).

BC is considered as a light absorbing carbonaceous component in particulate matter (Lack et al., 2014; Sasser et al., 2012). This characteristic classifies this pollutant as a contributor to climate change, changing the temperature profile at low atmosphere levels, frequency of the precipitations, surface albedo, and snow rate fusion. Several studies reported variations of climatic parameters using a combination of real monitoring and resulted from the simulation of numerical models (Bauer et al., 2013; Bond et al., 2007; Novakov et al., 2003; Wang et al., 2014). It is one of the short-lived climate pollutants.

The decrease in the particle size of BC increases the ability to stay in the air, which favors its transport over long distances (Waggoner et al., 2015). Due to limiting measurement sites across Antarctica, chemistry transport models can fill the cap. Research studies at local (Lyamani et al., 2011; Srivastava et al., 2012), regional (Gertler et al., 2016), continental (Briggs and Long, 2016), and global scale (Ramanathan and Carmichael, 2008) have simulated atmospheric BC dispersion. This information could be obtained using air quality simulation models. These are computational tools that act as surrogate atmospheres in those locations where experimentation is not possible. They are designed by the combination of mathematical equations and results of experiments that correspond to appropriate solutions for them. These computational tools have different levels of complexity to obtain results.

The development of air quality simulation during the last decade allowed the presence of BC in remote zones of the planet like the Arctic (Cheng, 2014; Gogoi et al., 2016; Huang et al., 2015a; Zhou et al., 2012), Himalaya's mountains (Bhat et al., 2017; Gertler et al., 2016; Negi et al., 2019; Yasunari et al., 2013) glaciers of North America (Hanna et al., 2018), and rural areas of Asia (Cheng, 2014; Ming et al., 2013; Wang et al., 2016; Winther et al., 2014). The first study using an air quality model (Penner et al., 1993) wich domain simulated the air of Antarctica considered the biomass burning emissions from Brazil, Australia, Indonesia, and Africa as the primary external source. That research estimated an anthropogenic BC emission inventory using BC to sulfur dioxide (SO_2) ratio and SO_2 global emissions and included biomas burning emissions from previous reports. Using a Lagrangian parcel model called GRANDTOUR, they simulated the long transportation of BC on January and July with a 4.5 × 7.5° grid resolution and compared the results with measured observations worldwide, including only one site with available records in the South Pole. In this specific location, the predicted value of atmospheric BC was 0.2 ng/m^3 and 0.14 ng/m^3 on January and July, respectively, and both records were lower than measured concentrations. The difference was associated with the underprediction of the biomass burning emissions. Meanwhile, air monitoring campaign results (Hansen et al., 2001) registered a strong local effect in McMurdo station, another zone of Antarctica, during November 1995 and February 1996. A similar pattern was observed for the same period in the results of the air monitoring campaign reported by Pereira et al. (2006), but this study confirmed the simulated results of Penner et al. in the comparison at the South Shetland Islands, Antarctic Peninsula. They showed a direct correlation of the biomass burning activity in Southern Hemisphere and atmospheric BC anomalies measurements applying principal component analysis with BC, Radon element and meteorological data. It is remarkable to distinguish that studies reported many wildfires every year (Buergelt and Smith, 2015; dos Santos et al., 2019; Fischer et al., 2012; Huang et al., 2015b; Jaffe and Wigder, 2012; Úbeda and Sarricolea, 2016) in those regions that geographically surround the Antarctic Continent.

The study reported by Asmi et al. (2018) measured equivalent BC mass fractions by optical means showing an average of 17.3 ng/m^3 at the Marambio station, considered as higher than other published studies, and those authors treated local influences from the Antarctic Peninsula in the results. However, an analysis of two ice core records by Arienzo et al. (2017) showed a similar conclusion mentioned in the last paragraph. Also, through a combination of snow and satellite analysis, most recent results (Khan et al., 2019) concluded that local and external emissions impacted the deposition of atmospheric BC in Antarctica. A similar conclusion was reported by Hara et al. (2019) at the Syowa station using atmospheric BC samples and back-trajectory simulations in the period of February 2005 – December 2016, and the study published by Marquetto et al. (2020) analyzing the 2014–2015 Austral summer on the Pine Island Glacier with the same approach. Nonetheless, an updated global atmospheric BC apportionment of all sources in the complete region of Antarctica has not been reported. Thus, we were able to expose a hemispheric simulation of Southern Hemisphere emissions and evaluate the effect of those sources in the atmospheric BC concentration to Antarctica.

2. Methodology

2.1. Modeling system and simulation inputs

The model Weather Research Forecast (WRF) version 3.7.1 was used for meteorological simulation (Skamarock et al., 2008). The polar stereographic projection was chosen, centered on Antarctica at coordinates −90° South and −65.523° West, same as reported by Pino-Cortés et al. (2020a). The domain of the study was set in 180 × 180 grid cells and a resolution of 108 km, the same as published by other studies with an emphasis on simulation of air quality in the hemispheric analysis (Huang et al., 2015a; Sarwar et al., 2019). The geographical resolution was set in 10 min, with 50 vertical layers. The input files of the meteorological variables were downloaded from the Nation Center for Atmospheric Research Data Archive (NCAR RDA) website (rda.ucar.edu/) type GRIB2, option ds0.83.3 (NCEP, 2015) from January 1st to May 1st of 2014. The parameterization used for the meteorological simulation is shown in Table 1.

The emission inventory required for air quality simulation was processed using Sparse Matrix Operator Kernel Emissions (SMOKE) model, version 4.5 (Baek and Seppanen, 2018). The specific details of the module's processing and steps made in SMOKE are explained in the previous report (Pino-Cortés et al., 2020a). The anthropogenic emissions in Southern Hemisphere is challenging to obtain due to the lack of national information disaggregated geographically. The Emissions Database for Global Atmospheric Research (EDGAR), version HTAP2.2 (Janssens-Maenhout et al., 2015) was used as an input in SMOKE. EDGAR is a compiled source emission with results from ships (sea transportation), Energy (electric generation), Industry, Transport and Residential sectors. The biomass burning emission from wildfires is one of the main sources of atmospheric pollutants and it is considered the primary source of atmospheric BC and $PM_{2.5}$ worldwide (Bond et al., 2013). The development of an emissions inventory for this activity has been published in the last years. In this study, we used the Global Fire

Table 1
Settings of WRF3.7.1 for meteorological simulation.

Parameterization	Variable	Option	Reference
Microphysics	mp_physics	6	(Hong and Lim, 2006)
Radiation longwave	ra_lw_physics	3	(Collins et al., 2004)
Radiation shortwave	ra_sw_physics	3	(Collins et al., 2004)
Surface Layer	sf_sfclay_physics	1	(Jiménez et al., 2012)
Planetary Boundary Layer	bl_pbl_physics	5	(NAKANISHI and NIINO, 2009)
Cumulus	cu_physics	4	(Pan and Wu, 1995)

Assimilation System (GFAS) version 1.3 (Kaiser et al., 2012). The steps and implementation of this database for SMOKE use have been reported previously (Pino-Cortés et al., 2020b).

The Community Multiscale Air Quality model (CMAQ) version 5.2 (EPA, 2017) was used for atmospheric BC dispersion in Southern Hemisphere. The initial and boundary conditions were set to zero to avoid the effects of any particular value. Also, a spin-up period of 2 months (January–February 2014) was considered, being the target days between March and April in 2014, due to the long transportation of this pollutant in the air. Different scenarios were considered in CMAQ for source identification, including all sources and those without one source emissions.

2.2. Simulation outputs analysis

The meteorological simulation outputs and atmospheric BC dispersion from CMAQ were compared with satellite-based data. The results from the Modern-Era Retrospective Analysis for Research and Applications, version 2 (MERRA-2) database (Global Modelling and Assimilation Office, 2018) were considered as real observation for temperature, wind speed and atmospheric black carbon at surface level, due to the size of the grid cell (0.5° in horizontal and 0.625° in vertical) and the time step (1 h). That database is a NASA atmospheric reanalysis for the satellite era using the Goddard Earth Observing System Model, Version 5 (GEOS-5) with its Atmospheric Data Assimilation System. MERRA-2 registries have lower horizontal resolution than our results, but it records the most acceptable values for a hemispheric analysis. Many studies have compared and correlated the results from that database and the local measurement of meteorological variables and aerosols (Carmona et al., 2020; Hareef baba shaeb et al., 2020; Ma et al., 2019; Ren et al., 2020; Sitnov et al., 2020). The average Mean Bias (MB), Normalized Mean Bias (NMB) and Index of Agreement (IOA) were used as the main statistical operators for model outputs validation of the average daily results and their definitions have been published (Emery et al., 2001).

3. Results and discussion

The atmospheric BC emissions were analyzed between January and May of 2014, being the biomass burning the primary source in the Southern Hemisphere during that period. We studied the monthly profile emissions for the most relevant or populated cities in this domain (Fig. 1). The higher monthly registries were observed in January for biomass burning, except in Temuco, Chile, where the highest emission was observed in March. The anthropogenic emissions were similar during the period of analysis for all the cities studied. The results from Bloemfontein, South Africa, were the highest emissions of black carbon, which is more than double of the results observed in Santiago de Chile, the capital of Chile, and Rio de Janeiro and Sao Paulo, both the most populated and largest cities in Brazil. The low registries observed in the cities of Australia and New Zealand for biomass burning and anthropogenic sources are remarkable. Most details of the black carbon emissions in the Southern Hemisphere for both sectors in a hemispheric analysis are reported in other studies (Pino-Cortés et al., 2020b, 2020a). It is remarkable to distinguish that future modeling studies must consider the different types of BC from the sources of generation. Hygroscopic biomass smoke may be susceptible to the uptake of water vapor during transport through high-humidity areas: leading to possible incorporation into cloud droplets and eventual removal by precipitation. On the other hand, hydrophobic diesel exhaust may be able to avoid nucleation and travel longer distances. This kind of distinction is not possible in CMAQ.

Simulated surface daily concentrations of black carbon from March 1st to April 30th of 2014 were obtained and analyzed. The values reported in the Modern-Era Retrospective Analysis for Research and Applications (MERRA-2) (Gelaro et al., 2017) were assumed as observational registries to analyze the time series obtained. Our attention was centered in fifteen coastal zones of Antarctica (Fig. 2, Table 2), where scientific bases and inhabitants are present. More locations with the same information can be observed in Supplementary information (Table S1).

Similar values were observed and acceptable performance was obtained in the period of analysis. The mean daily concentrations of BC obtained in CMAQ showed in most locations an average IOA in the range of 0.–0.5 except for Smyley, Syowa, Thurston and Yelcho, where IOA was lower. The negative values of the NMB show the low underprediction of the concentrations simulated by CMAQ, but acceptable for the hemispheric approach. The average simulated value obtained in Syowa is lower than the 2.7 ng/m^3 reported by (Hara et al., 2019) during the same period, but the satellite registry is statistically identical. In other hand, the CMAQ output and satellite values in Marambio are six times lower than the average reported by Asmi et al. (2018) during 2013–2015. Unfortunately, in this study we did not find more available time series of atmospheric BC from the monitoring stations placed in Antarctica for the model comparison. Also, the grid size resolution of the domain is higher than the resolution of the equipment used for atmospheric BC measurement.

The average daily black carbon concentrations were under 4 ng/m^3, but some peaks in most of the zones from MERRA-2 registries were not replicated by CMAQ output on different days, as observed in Fig. 2. We mainly associated those peaks with emissions not considered on specific days before. This assumption has been argued in other hemispheric studies (Chen et al., 2018; Huang et al., 2015a) and it is mainly related to the low reactivity of the black carbon in the air. It is remarkable to say that the emissions from ships are always present and surrounding Antarctica, but there are lower than biomass burning and other anthropogenic sources from the continents.

The low concentrations of black carbon in the air of Antarctica are associated with its pristine environment characteristics. Therefore, CMAQ considers the same concentration in the horizontal grid resolution of the

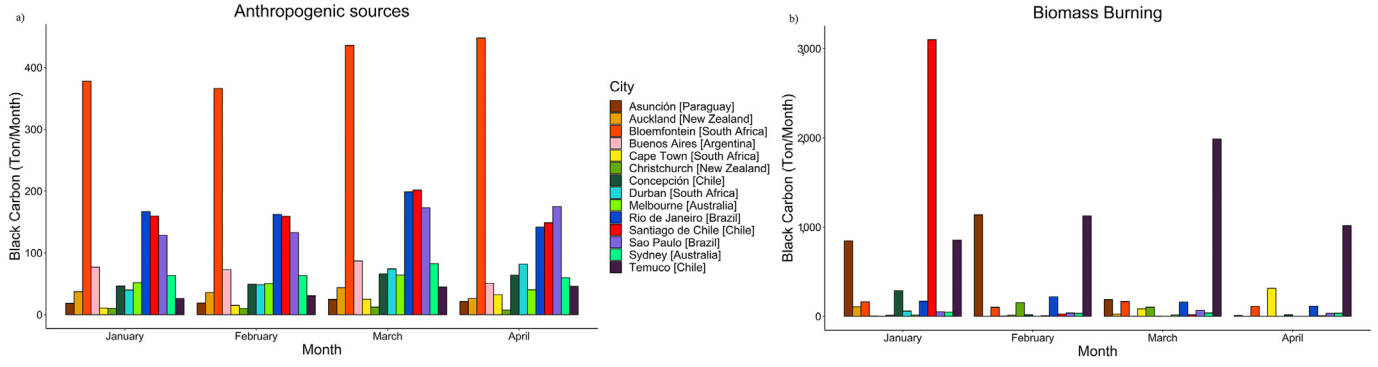

Fig. 1. BC emissions during January and April of 2014 at the most important cities in Southern Hemisphere from a) anthropogenic b) biomass burning.

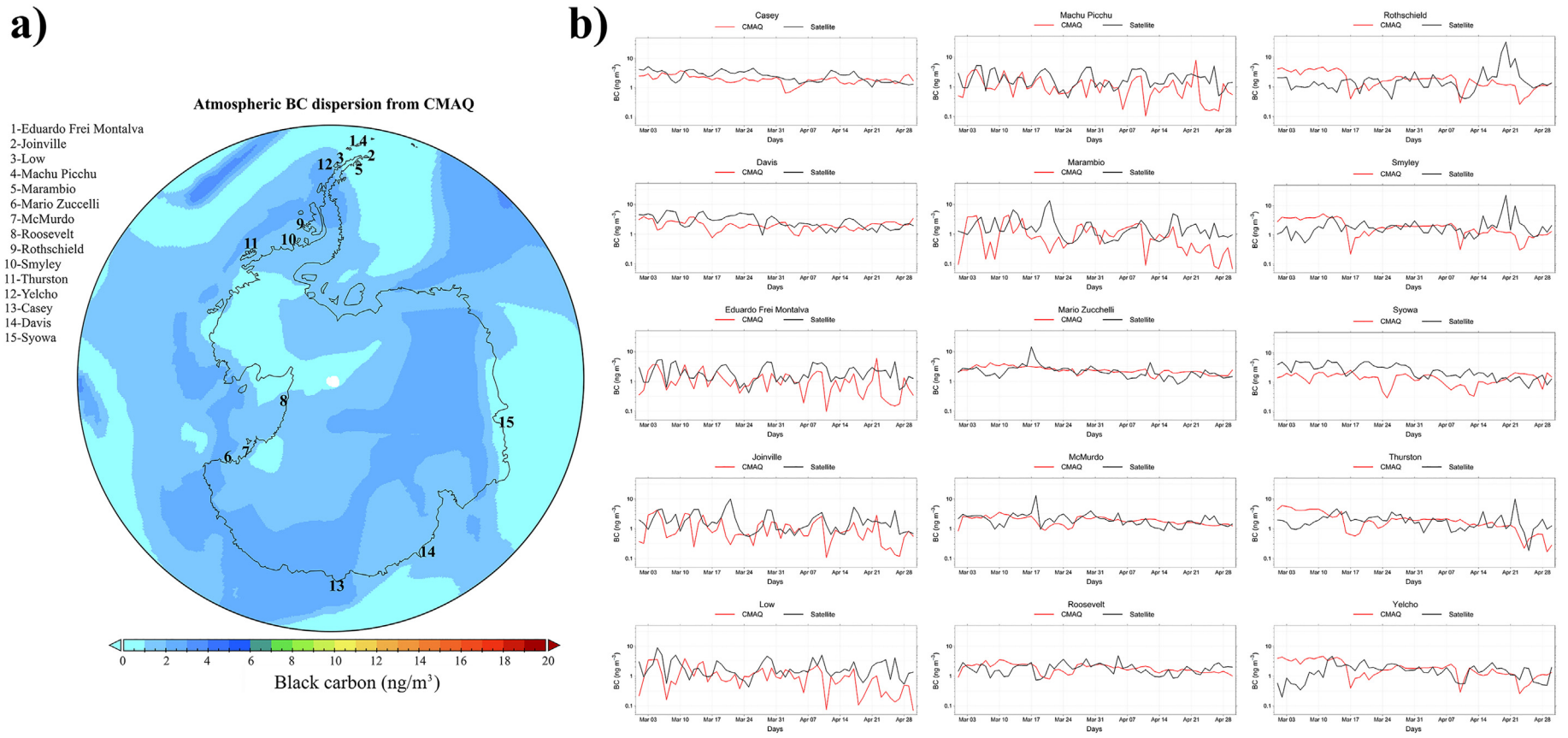

Fig. 2. Comparison of atmospheric black carbon concentrations from CMAQ and MERRA-2. a) Registries in Antarctica on April 15th, 2014. b) Daily concentrations in fifteen zones in Antarctica.

Table 2
Summary of mean atmospheric BC concentrations and simulated output validation.

Location	Mean BC (ng/m^3)		IOA	NMB	MB
	CMAQ	MERRA-2			
Casey	1.968	2.642	0.4258	−0.2549	−0.6735
Davis	2.058	2.876	0.4323	−0.2846	−0.8185
Eduardo Frei Montalva	1.224	2.103	0.4160	−0.4177	−0.8784
Joinville	1.127	2.022	0.4765	−0.4427	−0.8952
Low	1.106	2.043	0.4295	−0.4584	−0.9364
Machu Picchu	1.260	2.106	0.4198	−0.4020	−0.8468
Marambio	1.111	1.920	0.4184	−0.4215	−0.8092
Mario Zucchelli	2.402	2.343	0.5035	0.0251	0.0589
McMurdo	1.902	2.186	0.5049	−0.1298	−0.2837
Roosevelt	1.876	1.863	0.3998	0.0074	0.0138
Rothschield	1.959	2.307	0.4279	−0.1510	−0.3484
Smyley	2.016	2.274	0.3672	−0.1136	−0.2583
Syowa	1.388	2.657	0.3482	−0.4776	−1.2695
Thurston	2.065	1.943	0.1822	0.0626	0.1216
Yelcho	1.959	1.562	0.1581	0.2541	0.3969

domain. It means equal value in 108 km^2, which is the grid cell size in this study. This issue was also exposed by Penner et al. (1993) when lower BC simulated values were compared in coastal zones and the sea conditions are dominant due to the resolution of the domain. In this sense, future simulations must analyze the mesoscale resolution in Antarctica, considering nested domains for long transportation from the continent to the sites of the study. Also, that scenario must consider the local anthropogenic emissions, such as combustion waste treatment, power and heat generation, and transportation in the Antarctica stations that have been exposed in previous studies (Hansen et al., 2001; Khan et al., 2018; Pereira et al., 2006; Sheridan et al., 2016). Unfortunately, this study did not include those registries due to the lack of information, and it could be another cause for the daily difference between CMAQ and MERRA-2 registries.

The advantages of the air quality simulation are to bring answers to unsolved questions like the main responsible for atmospheric black carbon concentrations in Antarctica. In this study, we made a simulation without considering biomass burning emissions between March 1st and April 30th of 2014. The effect of this source emission is considerable, and it is shown in Fig. 3.

The average daily atmospheric black carbon concentrations decreased in the range of 20–50% when the scenario without biomass burning was considered (for other zones details, see Fig. S3). The results indicate that the CMAQ model simulated the transport of BC from lower latitudes and showed the direct effect of this source on the atmospheric black carbon concentrations in the Antarctic continent. It probes conclusions mentioned in monitoring campaigns at specific locations like Pine Island Glacier (Marquetto et al., 2020), King George Island (Pereira et al., 2006), Zhongshan (Ma et al., 2020) Palmer (Khan et al., 2019), and O'Higgins (Cereceda-Balic et al., 2020) base stations. The most relevant finding of this study is the simulation of the hemispheric transportation of atmospheric black carbon particles from Southern continents to Antarctica and both anthropogenic and biomass burning emissions sources effect. Even when the natural circumpolar wind prevents the ingress of airmasses from lower latitudes particles in Austral winter, this effect is reduced in late spring and weaker during summer in Southern Hemisphere (Waugh et al., 2017). It is highly probably the long transportation of particles during that period and higher surface concentrations of BC in Antarctica during late summer.

The daily average BC concentrations without biomass burning emissions throw simulation were analyzed in Fig. 4. The real effect of this source showed evidence after 17 days when the registries started to decrease compared to the simulation with all emissions sources. The locations with the highest difference were those located nearest to Australia and New Zealand, like McMurdo, Mario Zucchelli and Roosevelt. These zones in Antarctica must be affected by the westerly wind transport of atmospheric BC from the several yearly wildfires emissions that occurred in both countries.

On the other side, a middle difference was observed in Thurston, Rothschild and Smiley locations, which is expected. Those stations are on the West side of Antarctica and far from the continents. In this region, the atmospheric BC particles showed significant difference past 24 days since the biomass burning emissions were shutdown, which also evidences the effect of this source. A similar trend was observed in isolated stations like Casey, Davis and Syowa. Finally, the rest of the studied locations showed a lower difference in atmospheric BC concentrations. Otherwise, the original peak registry in Eduardo Frei Montalva, Macchu Picchu and Joinville on April 22nd was not replicated in the second scenario. This anomaly was not observed in other nearby locations like

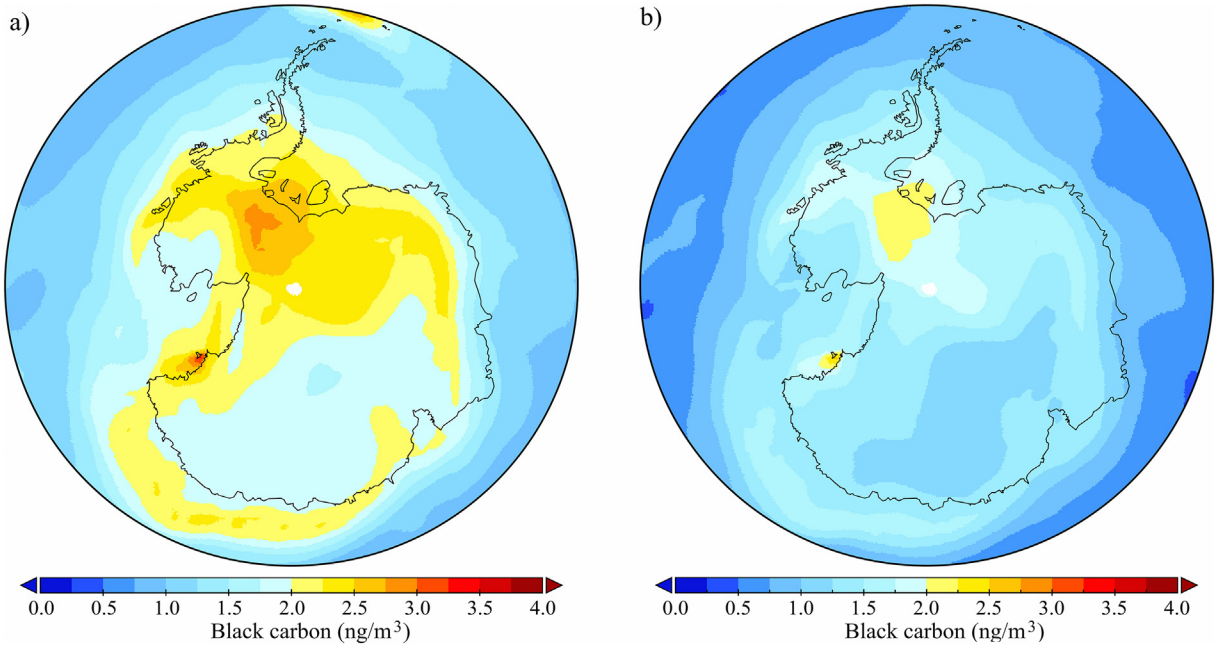

Fig. 3. Average simulated BC concentrations from March 1st to April 30th of 2014. a) All sources emissions considered. b) Without biomass burning emissions considered.

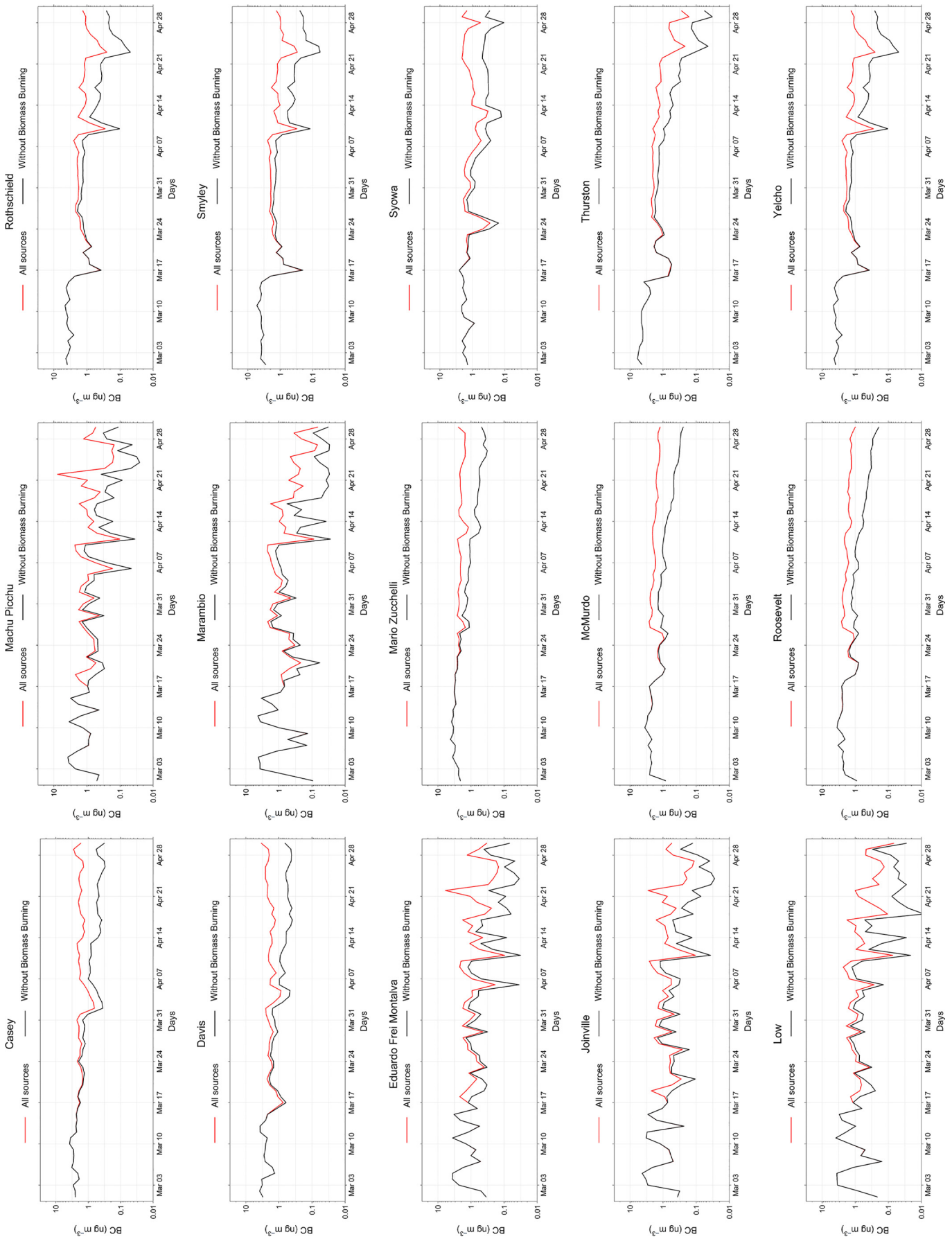

Fig. 4. Comparison of daily black carbon concentrations with and without biomass burning emissions.

Marambio, Yelcho and Low stations. The statistical analysis of biomass burning emissions effect in Antarctica was stated in Supplementary files. We considered that the orography in these zones of Antarctica could affect the wind direction, deviating the atmospheric BC particles from Southern America to specific locations in some period.

4. Conclusions

We simulated the dispersion of atmospheric black carbon emissions from the Southern Hemisphere and compared the results with satellite registries during the late summer of 2014, when the tropospheric polar vortex is weak This research showed the effect of biomass burning emissions in Antarctica, with 17–20 days of transportation from land to the continent. Otherwise, the main results suggest that the hemispheric analysis of atmospheric black carbon dispersion must keep studying for future scenarios. Also, particle speciation in a mesoscale analysis must include the local anthropogenic sources of the research stations for better known on specific locations of the continent. Long-range transport brings other aerosol species of anthropogenic/combustion origin, such as sulfates and nitrates which may affect snow composition, melting point, and albedo. . Even when the average air concentration of atmospheric BC in Antarctica is relatively low (under 4 ng/m^3), an intensification of the natural and anthropogenic emissions of atmospheric BC could increase the future climate trends in West Antarctica. That is why more public policies must address efficient climate change strategies to prevent and reduce wildfires in the Southern Hemisphere. The uncontrolled emissions of black carbon can increase the probability of its transportation to the white and pristine continent and produce its accumulation,This scenario could consequently impact on the acceleration in the melting of snow and ice, the change in the albedo of this area of the cryosphere and significantly affect the earth's radiative balance, aggravating the global climate change.

Funding

This work was supported by ANID BECAS/DOCTORADO NACIONAL 21150125, ANID FONDECYT 112079 and the supercomputing infrastructure at NLHPC (ECM-02). This work was funded also by the Chilean Ministry of Science, Technology, Knowledge and Innovation under projects FONDEF ID18I10152 and FONDEF ID19I10359 and by Universidad Técnica Federico Santa María under project DGIIP PI_M_2020_58.

Credit authorship contribution statement

Ernesto Pino-Cortés, **Luis Díaz-Robles**, **Francisco Cereceda-Balic** and **Joshua S. Fu** conceived the study, conducted the simulations and wrote the initial draft of the paper. **Francisco Cubillos** and **Roberto Santander** reviewed and refined the initial draft of the paper. **Samuel Carrasco** and **Jonathan Acosta** analyzed the statistical performance. All authors contributed to interpreting the results and refinement of the paper.

Data availability

The other data that support the findings of this study are available from the corresponding author upon reasonable request.

Code availability

The WRF version 3.7.1 codes can be downloaded at wrf/users/download/get_source.html. The CMAQ version 5.2 codes can be downloaded at www.cmascenter.org. Maps used in the spatial plots were created using Panoply and it is available at www.giss.nasa.gov/tools/panoply. The map used in the graphical abstract was built in Vapor and this software can be downloaded at www.vapor.ucar.edu.

Declaration of competing interest

The authors declare no competing interests.

Acknowledgments

We acknowledge ECCAD for the archiving and distribution of the data EDGAR and GFASv1.3.

Appendix A. Supplementary data

Supplementary data to this article can be found online at https://doi.org/10.1016/j.scitotenv.2021.146242.

References

Arienzo, M.M., McConnell, J.R., Murphy, L.N., Chellman, N., Das, S., Kipfstuhl, S., Mulvaney, R., 2017. Holocene black carbon in Antarctica paralleled southern hemisphere climate. J. Geophys. Res. Atmos. 122, 6713–6728. https://doi.org/10.1002/2017JD026599.

Asmi, E., Neitola, K., Teinilä, K., Rodriguez, E., Virkkula, A., Backman, J., Bloss, M., Jokela, J., Lihavainen, H., de Leeuw, G., Paatero, J., Aaltonen, V., Mei, M., Gambarte, G., Copes, G., Albertini, M., Fogwill, G.P., Ferrara, J., Barlasina, M.E., Sánchez, R., 2018. Primary sources control the variability of aerosol optical properties in the Antarctic Peninsula. Tellus Ser. B Chem. Phys. Meteorol. 70, 1–16. https://doi.org/10.1080/16000889.2017.1414571.

Baek, B.H., Seppanen, C., 2018. Spare Modeling Operator Kerner Emissions (SMOKE) Modeling System. https://doi.org/10.5281/ZENODO.1421403.

Bauer, S.E., Bausch, A., Nazarenko, L., Tsigaridis, K., Xu, B., Edwards, R., Bisiaux, M., McConnell, J., 2013. Historical and future black carbon deposition on the three ice caps: ice core measurements and model simulations from 1850 to 2100. J. Geophys. Res. Atmos. 118, 7948–7961. https://doi.org/10.1002/jgrd.50612.

Bhat, M.A., Romshoo, S.A., Beig, G., 2017. Aerosol black carbon at an urban site-Srinagar, northwestern Himalaya, India: seasonality, sources, meteorology and radiative forcing. Atmos. Environ. 165, 336–348. https://doi.org/10.1016/j.atmosenv.2017.07.004.

Bond, T.C., Bhardwaj, E., Dong, R., Jogani, R., Jung, S., Roden, C., Streets, D.G., Trautmann, N.M., 2007. Historical emissions of black and organic carbon aerosol from energy-related combustion, 1850-2000. Global Biogeochem. Cycles 21. https://doi.org/10.1029/2006GB002840 (n/a-n/a).

Bond, T.C., Doherty, S.J., Fahey, D.W., Forster, P.M., Berntsen, T., DeAngelo, B.J., Flanner, M.G., Ghan, S., Kärcher, B., Koch, D., Kinne, S., Kondo, Y., Quinn, P.K., Sarofim, M.C., Schultz, M.G., Schulz, M., Venkataraman, C., Zhang, H., Zhang, S., Bellouin, N., Guttikunda, S.K., Hopke, P.K., Jacobson, M.Z., Kaiser, J.W., Klimont, Z., Lohmann, U., Schwarz, J.P., Shindell, D., Storelvmo, T., Warren, S.G., Zender, C.S., 2013. Bounding the role of black carbon in the climate system: a scientific assessment. J. Geophys. Res. Atmos. 118, 5380–5552. https://doi.org/10.1002/jgrd.50171.

Briggs, N.L., Long, C.M., 2016. Critical review of black carbon and elemental carbon source apportionment in Europe and the United States. Atmos. Environ. 144, 409–427. https://doi.org/10.1016/j.atmosenv.2016.09.002.

Buergelt, P.T., Smith, R., 2015. Chapter 6 - wildfires: an Australian perspective. In: Shroder, J.F. (Ed.), Paton Risks and Disasters, D.B.T.-W.H. Elsevier, Oxford, pp. 101–121 https://doi.org/10.1016/B978-0-12-410434-1.00006-3.

Carmona, J.M., Gupta, P., Lozano-García, D.F., Vanoye, A.Y., Yépez, F.D., Mendoza, A., 2020. Spatial and temporal distribution of PM2.5 pollution over northeastern Mexico: application of MERRA-2 reanalysis datasets. Remote Sens. 12, 2286. https://doi.org/10.3390/rs12142286.

Cereceda-Balic, F., Vidal, V., Ruggeri, M.F., González, H.E., 2020. Black carbon pollution in snow and its impact on albedo near the Chilean stations on the Antarctic peninsula: first results. Sci. Total Environ. 743, 140801. https://doi.org/10.1016/j.scitotenv.2020.140801.

Chen, X., Kang, S., Cong, Z., Yang, J., Ma, Y., 2018. Concentration, temporal variation, and sources of black carbon in the Mt. Everest region retrieved by real-time observation and simulation. Atmos. Chem. Phys. 18, 12859–12875. https://doi.org/10.5194/acp-18-12859-2018.

Cheng, M.D., 2014. Geolocating Russian sources for Arctic black carbon. Atmos. Environ. 92, 398–410. https://doi.org/10.1016/j.atmosenv.2014.04.031.

Collins, W.D., Rasch, P.J., Boville, B.A., McCaa, J., Williamson, D.L., Kiehl, J.T, et al., 2004. Description of the NCAR Community Atmosphere Model (CAM 3.0) (No. NCAR/TN-464+STR). University Corporation for Atmospheric Research https://doi.org/10.5065/D63N21CH https://opensky.ucar.edu/islandora/object/technotes%3A477/datastream/PDF/view.

dos Santos, J.F.C., Gleriani, J.M., Velloso, S.G.S., de Souza, G.S.A., do Amaral, C.H., Torres, F.T.P., Medeiros, N.D.G., dos Reis, M., 2019. Wildfires as a major challenge for natural regeneration in Atlantic Forest. Sci. Total Environ. 650, 809–821. https://doi.org/10.1016/j.scitotenv.2018.09.016.

Emery, C.A., Tai, E., Yarwood, G., 2001. Enhanced meteorological modeling and performance evaluation for two Texas ozone episodes. Enhanc. Meteorol. Model. Perform. Eval. Two Texas Ozone Episodes.

EPA, U, 2017. CMAQ (Version 5.2). https://doi.org/10.5281/ZENODO.1167892.

Fischer, M.A., Di Bella, C.M., Jobbágy, E.G., 2012. Fire patterns in central semiarid Argentina. J. Arid Environ. 78, 161–168. https://doi.org/10.1016/j.jaridenv.2011.11.009.

Gelaro, R., McCarty, W., Suárez, M.J., Todling, R., Molod, A., Takacs, L., Randles, C.A., Darmenov, A., Bosilovich, M.G., Reichle, R., Wargan, K., Coy, L., Cullather, R., Draper, C., Akella, S., Buchard, V., Conaty, A., da Silva, A.M., Gu, W., Kim, G.-K., Koster, R., Lucchesi, R., Merkova, D., Nielsen, J.E., Partyka, G., Pawson, S., Putman, W., Rienecker, M., Schubert, S.D., Sienkiewicz, M., Zhao, B., 2017. The modern-era retrospective analysis for research and applications, version 2 (MERRA-2). J. Clim. 30, 5419–5454. https://doi.org/10.1175/JCLI-D-16-0758.1.

Gertler, C.G., Puppala, S.P., Panday, A., Stumm, D., Shea, J., 2016. Black carbon and the Himalayan cryosphere: a review. Atmos. Environ. 125, 404–417. https://doi.org/10.1016/j.atmosenv.2015.08.078.

Global Modelling and Assimilation Offfice, 2018. MERRA-2 re-Analysis [WWW Document]. Web site URL. http://www.soda-pro.com/web-services/meteo-data/merra.

Gogoi, M.M., Babu, S.S., Moorthy, K.K., Thakur, R.C., Chaubey, J.P., Nair, V.S., 2016. Aerosol black carbon over Svalbard regions of Arctic. Polar Sci. 10, 60–70. https://doi.org/10.1016/j.polar.2015.11.001.

Hanna, S.J., Xu, J.-W., Schroder, J.C., Wang, Q., McMeeking, G.R., Hayden, K., Leaitch, W.R., Macdonald, A., von Salzen, K., Martin, R.V., Bertram, A.K., 2018. Refractory black carbon at the whistler peak high elevation research site – measurements and simulations. Atmos. Environ. 181, 34–46. https://doi.org/10.1016/j.atmosenv.2018.02.041.

Hansen, A.D.A., Lowenthal, D.H., Chow, J.C., Watson, J.G., 2001. Black carbon aerosol at McMurdo Station, Antarctica. J. Air Waste Manage. Assoc. 51, 593–600. https://doi.org/10.1080/10473289.2001.10464283.

Hara, K., Sudo, K., Ohnishi, T., Osada, K., Yabuki, M., Shiobara, M., Yamanouchi, T., 2019. Seasonal features and origins of carbonaceous aerosols at Syowa Station, coastal Antarctica. Atmos. Chem. Phys. 19, 7817–7837. https://doi.org/10.5194/acp-19-7817-2019.

Hareef baba shaeb, K., Biswadip, G., Dutta, D., Choudhury, S.B., Seshasai, M.V.R., 2020. Spatial variability of the aerosol optical thickness over Southern Ocean and coastal Antarctica: comparison with MODIS and MERRA-2 aerosol products. Deep Sea Res. Part II Top. Stud. Oceanogr. 178, 104776. https://doi.org/10.1016/j.dsr2.2020.104776.

Hong, S., Lim, J., 2006. The WRF Single-Moment 6-Class microphysics scheme (WSM6). Journal of the Korean Meteorological Society 42, 129–151.

Huang, K., Fu, J.S., Prikhodko, V.Y., Storey, J.M., Romanov, A., Hodson, E.L., Cresko, J., Morozova, I., Ignatieva, Y., Cabaniss, J., 2015a. Russian anthropogenic black carbon: emission reconstruction and Arctic black carbon simulation. J. Geophys. Res. Atmos. 120, 11,306–311,333. https://doi.org/10.1002/2015JD023358.

Huang, Y., Wu, S., Kaplan, J.O., 2015b. Sensitivity of global wildfire occurrences to various factors in the context of global change. Atmos. Environ. 121, 86–92. https://doi.org/10.1016/j.atmosenv.2015.06.002.

Jaffe, D.A., Wigder, N.L., 2012. Ozone production from wildfires: a critical review. Atmos. Environ. 51, 1–10. https://doi.org/10.1016/j.atmosenv.2011.11.063.

Janssens-Maenhout, G., Crippa, M., Guizzardi, D., Dentener, F., Muntean, M., Pouliot, G., Keating, T., Zhang, Q., Kurokawa, J., Wankmüller, R., Denier Van Der Gon, H., Kuenen, J.J.P., Klimont, Z., Frost, G., Darras, S., Koffi, B., Li, M., 2015. HTAP-v2.2: a mosaic of regional and global emission grid maps for 2008 and 2010 to study hemispheric transport of air pollution. Atmos. Chem. Phys. 15, 11411–11432. https://doi.org/10.5194/acp-15-11411-2015.

Jiménez, P.A., Dudhia, J., González-Rouco, J.F., Navarro, J., Montávez, J.P, García-Bustamante, E., 2012. A revised scheme for the WRF surface layer formulation. Monthly Weather Review 140 (3), 898–918. https://doi.org/10.1175/MWR-D-11-00056.1.

Kaiser, J.W., Heil, A., Andreae, M.O., Benedetti, A., Chubarova, N., Jones, L., Morcrette, J.-J., Razinger, M., Schultz, M.G., Suttie, M., van der Werf, G.R., 2012. Biomass burning emissions estimated with a global fire assimilation system based on observed fire radiative power. Biogeosciences 9, 527–554. https://doi.org/10.5194/bg-9-527-2012.

Khan, A.L., McMeeking, G.R., Schwarz, J.P., Xian, P., Welch, K.A., Berry Lyons, W., McKnight, D.M., 2018. Near-surface refractory black carbon observations in the atmosphere and snow in the McMurdo dry valleys, Antarctica, and potential impacts of Foehn winds. J. Geophys. Res. Atmos. 123, 2877–2887. https://doi.org/10.1002/2017JD027696.

Khan, A.L., Klein, A.G., Katich, J.M., Xian, P., 2019. Local emissions and regional wildfires influence refractory black carbon observations near Palmer Station, Antarctica. Front. Earth Sci. 7, 49.

Lack, D.A., Moosmüller, H., McMeeking, G.R., Chakrabarty, R.K., Baumgardner, D., 2014. Characterizing elemental, equivalent black, and refractory black carbon aerosol particles: a review of techniques, their limitations and uncertainties. Anal. Bioanal. Chem. 406, 99–122. https://doi.org/10.1007/s00216-013-7402-3.

Lyamani, H., Olmo, F.J., Foyo, I., Alados-Arboledas, L., 2011. Black carbon aerosols over an urban area in South-Eastern Spain: changes detected after the 2008 economic crisis. Atmos. Environ. 45, 6423–6432. https://doi.org/10.1016/j.atmosenv.2011.07.063.

Ma, J., Zhang, T., Guan, X., Hu, X., Duan, A., Liu, J., 2019. The dominant role of snow/ice albedo feedback strengthened by black carbon in the enhanced warming over the Himalayas. J. Clim. 32, 5883–5899. https://doi.org/10.1175/JCLI-D-18-0720.1.

Ma, X., Li, C., Du, Z., Dou, T., Ding, M., Ming, J., Wang, M., Gao, S., Xiao, C., Wang, X., Ren, J., Kang, S., 2020. Spatial and temporal variations of refractory black carbon along the transect from Zhongshan Station to Dome A, eastern Antarctica. Atmos. Environ. 242, 117816. https://doi.org/10.1016/j.atmosenv.2020.117816.

Marquetto, L., Kaspari, S., Cardia Simões, J., 2020. Refractory black carbon (rBC) variability in a 47-year West Antarctic snow and firn core. Cryosph. 14, 1537–1554. https://doi.org/10.5194/tc-14-1537-2020.

Ming, J., Xiao, C., Du, Z., Yang, X., 2013. An overview of black carbon deposition in high Asia glaciers and its impacts on radiation balance. Adv. Water Resour. 55, 80–87. https://doi.org/10.1016/j.advwatres.2012.05.015.

Nakanishi, M., Niino, H., 2009. Development of an Improved Turbulence Closure Model for the Atmospheric Boundary Layer. J. Meteor. Soc. Japan 87 (5), 895–912. https://doi.org/10.2151/jmsj.87.895.

NCEP, U.S.D. of C, 2015. NCEP GDAS/FNL 0.25 Degree Global Tropospheric Analyses and Forecast Grids.

Negi, P.S., Pandey, C.P., Singh, N., 2019. Black carbon aerosols in the ambient air of Gangotri glacier valley of north-western Himalaya in India. Atmos. Environ. 214, 116879. https://doi.org/10.1016/j.atmosenv.2019.116879.

Novakov, T., Ramanathan, V., Hansen, J.E., Kirchstetter, T.W., Sato, M., Sinton, J.E., Sathaye, J.A., 2003. Large historical changes of fossil-fuel black carbon aerosols. Geophys. Res. Lett. 30. https://doi.org/10.1029/2002GL016345.

Pan, H.L., Wu, W.S., 1995. Implementing a mass flux convection parameterization package for the NMC medium-range forecast model. NMC office note 409.40, 20–233. https://www2.mmm.ucar.edu/wrf/users/physics/phys_refs/CU_PHYS/Old_SAS.pdf.

Penner, J.E., Eddleman, H., Novakov, T., 1993. Towards the development of a global inventory for black carbon emissions. Atmos. Environ. Part A. Gen. Top. 27, 1277–1295. https://doi.org/10.1016/0960-1686(93)90255-W.

Pereira, E.B., Evangelista, H., Pereira, K.C.D., Cavalcanti, I.F.A., Setzer, A.W., 2006. Apportionment of black carbon in the South Shetland Islands, Antartic Peninsula. J. Geophys. Res. Atmos. 111, 1–14. doi:https://doi.org/10.1029/2005JD006086.

Petzold, A., Ogren, J.A., Fiebig, M., Laj, P., Li, S.M., Baltensperger, U., Holzer-Popp, T., Kinne, S., Pappalardo, G., Sugimoto, N., Wehrli, C., Wiedensohler, A., Zhang, X.Y., 2013. Recommendations for reporting black carbon measurements. Atmos. Chem. Phys. 13, 8365–8379. https://doi.org/10.5194/acp-13-8365-2013.

Pino-Cortés, E., Carrasco, S., Díaz-Robles, L.A., Cubillos, F., Cereceda-Balic, F., 2020a. Black and organic carbon fractions in fine particulate matter by sectors in the south hemisphere emissions for decision-making on climate change and health effects. Environ. Sci. Pollut. Res. https://doi.org/10.1007/s11356-020-10164-w.

Pino-Cortés, E., Carrasco, S., Díaz-Robles, L.A., Cubillos, F., Vallejo, F., Cereceda-Balic, F., Fu, J., 2020b. Emission Inventory Processing of Biomass Burning From A Global Dataset for Air Quality Modeling. https://doi.org/10.20944/PREPRINTS202008.0335.V1.

Ramanathan, V., Carmichael, G., 2008. Global and regional climate changes due to black carbon. Nat. Geosci. 1, 221.

Ren, L., Yang, Y., Wang, H., Zhang, R., Wang, P., Liao, H., 2020. Source attribution of Arctic black carbon and sulfate aerosols and associated Arctic surface warming during 1980–2018. Atmos. Chem. Phys. 20, 9067–9085. https://doi.org/10.5194/acp-20-9067-2020.

Sarwar, G., Gantt, B., Foley, K., Fahey, K., Spero, T.L., Kang, D., Mathur, R., Foroutan, H., Xing, J., Sherwen, T., Saiz-Lopez, A., 2019. Influence of bromine and iodine chemistry on annual, seasonal, diurnal, and background ozone: CMAQ simulations over the Northern Hemisphere. Atmos. Environ. 213, 395–404. https://doi.org/10.1016/j.atmosenv.2019.06.020.

Sasser, E., Hemby, J., Adler, K., Anenberg, S., Bailey, C., Brockman, L., Frank, N., 2012. Report to Congress on Black Carbon.

Sheridan, P., Andrews, E., Schmeisser, L., Vasel, B., Ogren, J., 2016. Aerosol measurements at south pole: climatology and impact of local contamination. Aerosol Air Qual. Res. 16, 855–872. https://doi.org/10.4209/aaqr.2015.05.0358.

Sitnov, S.A., Mokhov, I.I., Likhosherstova, A.A., 2020. Exploring large-scale black-carbon air pollution over northern Eurasia in summer 2016 using MERRA-2 reanalysis data. Atmos. Res. 235, 104763. https://doi.org/10.1016/j.atmosres.2019.104763.

Skamarock, W.C., Klemp, J.B., J.D, Gill, D.O., D.M.B, Duda, M.G., X.-Y.H, Wang, W., Powers, J.G., 2008. A description of the advanced research WRF version 3. NCAR Tech. Note NCAR/TN-475+STR, 113 https://doi.org/10.5065/D68S4MVH.

Srivastava, A.K., Singh, S., Pant, P., Dumka, U.C., 2012. Characteristics of black carbon over Delhi and Manora peak—a comparative study. Atmos. Sci. Lett. 13, 223–230. https://doi.org/10.1002/asl.386.

Úbeda, X., Sarricolea, P., 2016. Wildfires in Chile: a review. Glob. Planet. Change 146, 152–161. https://doi.org/10.1016/j.gloplacha.2016.10.004.

Waggoner, D.C., Chen, H., Willoughby, A.S., Hatcher, P.G., 2015. Formation of black carbon-like and alicyclic aliphatic compounds by hydroxyl radical initiated degradation of lignin. Org. Geochem. 82, 69–76. https://doi.org/10.1016/j.orggeochem.2015.02.007.

Wang, R., Tao, S., Shen, H., Huang, Y., Chen, H., Balkanski, Y., Boucher, O., Ciais, P., Shen, G., Li, W., Zhang, Y., Chen, Y., Lin, N., Su, S., Li, B., Liu, J., Liu, W., 2014. Trend in global black carbon emissions from 1960 to 2007. Environ. Sci. Technol. 48, 6780–6787. https://doi.org/10.1021/es5021422.

Wang, Q., Huang, R.-J., Cao, J., Tie, X., Shen, Z., Zhao, S., Han, Y., Li, G., Li, Z., Ni, H., Zhou, Y., Wang, M., Chen, Y., Su, X., 2016. Contribution of regional transport to the black carbon aerosol during winter haze period in Beijing. Atmos. Environ. 132, 11–18. https://doi.org/10.1016/j.atmosenv.2016.02.031.

Waugh, D.W., Sobel, A.H., Polvani, L.M., 2017. What is the polar vortex and how does it influence weather? Bull. Am. Meteorol. Soc. 98, 37–44. https://doi.org/10.1175/BAMS-D-15-00212.1.

Winther, M., Christensen, J.H., Plejdrup, M.S., Ravn, E.S., Eriksson, Ó.F., Kristensen, H.O., 2014. Emission inventories for ships in the arctic based on satellite sampled AIS data. Atmos. Environ. 91, 1–14. https://doi.org/10.1016/j.atmosenv.2014.03.006.

Yasunari, T.J., Tan, Q., Lau, K.M., Bonasoni, P., Marinoni, A., Laj, P., Ménégoz, M., Takemura, T., Chin, M., 2013. Estimated range of black carbon dry deposition and the related snow albedo reduction over Himalayan glaciers during dry pre-monsoon periods. Atmos. Environ. 78, 259–267. https://doi.org/10.1016/j.atmosenv.2012.03.031.

Zhou, C., Penner, J.E., Flanner, M.G., Bisiaux, M.M., Edwards, R., McConnell, J.R., 2012. Transport of black carbon to polar regions: sensitivity and forcing by black carbon. Geophys. Res. Lett. 39. https://doi.org/10.1029/2012GL053388.